

DEVELOPMENT AND VALIDATION OF A CONGENER-SPECIFIC
PHOTODEGRADATION MODEL FOR POLYBROMINATED DIPHENYL ETHERSXIA ZENG,[†] STACI L. MASSEY SIMONICH,^{*†‡} KRISTIN R. ROBROCK,[§] PETER KORYTÁR,^{||} LISA ALVAREZ-COHEN,[§]
and DOUGLAS F. BAROFSKY[†][†]Department of Chemistry, [‡]Department of Environmental and Molecular Toxicology, Oregon State University, Corvallis, Oregon 97331, USA[§]Department of Civil and Environmental Engineering, University of California, Berkeley, California 94720, USA^{||}Wageningen Institute for Marine Resources and Ecosystem Studies, Haringkade 1, 1976 CP IJmuiden, The Netherlands

(Received 29 October 2007; Accepted 16 May 2008)

Abstract—With the phaseout of the manufacture of some polybrominated diphenyl ether (PBDE) formulations, namely penta-brominated diphenyl ether (BDE) and octa-BDE, and the continued use of the deca-BDE formulation, it is important to be able to predict the photodegradation of the more highly brominated congeners. A model was developed and validated to predict the products and their relative concentrations from the photodegradation of PBDEs. The enthalpies of formation of the 209 PBDE congeners were calculated, and the relative reaction rate constants were obtained. The predicted reaction rate constants for PBDEs show linear correlation with previous experimental results. Because of their large volume use, their presence in the environment, and/or importance in the photodegradation of the deca-BDE formulation, BDE-209, BDE-184, BDE-100, and BDE-99 were chosen for further ultraviolet photodegradation experiments in isooctane. The photodegradation model successfully predicted the products of the photochemical reactions of PBDEs in experimental studies. A gas chromatography retention time model for PBDEs was developed using a multiple linear regression analysis and, together with the photodegradation model and additional PBDE standards, provided a way to identify unknown products from PBDE photodegradation experiments. Based on the results of the photodegradation experiments, as well as the model predictions, it appears that the photodegradation of PBDEs is a first-order reaction and, further, that the rate-determining step is the stepwise loss of bromine. Our results suggest that, based on photodegradation, over time, BDE-99 will remain the most abundant penta-BDE, while BDE-49 and BDE-66 will increase greatly and will be comparable in abundance to BDE-47.

Keywords—Polybrominated diphenyl ether Photodegradation Model Theoretical calculation

INTRODUCTION

Polybrominated diphenyl ether (PBDE) flame retardants are widely used in consumer products to reduce flammability [1]. Increasing consumer use has led to increasing PBDE concentrations in the environment and the human body [2–5]. Because of their potential toxicity [6,7], the use of penta-brominated diphenyl ether (BDE) and octa-BDE formulations has been banned in Europe and voluntarily phased out in the United States [8]. However, with the continued use of the deca-BDE formulation, large quantities of PBDEs are still being released into the environment. The congener BDE-209, the major ingredient of deca-BDE technical mixture, has been reported to photodegrade under ultraviolet (UV) and natural sunlight to give lower PBDEs, including the banned penta-BDEs and octa-BDEs [9,10]. This finding has led to a need for a model to explain and predict the products of the photodegradation of PBDEs and their relative abundances. In our previous study, the enthalpies of formation of 39 PBDE congeners were calculated using Gaussian 03 (Revision B.05, Gaussian, Pittsburg, PA, USA) and a group additivity method (GAM) was developed [11]. This made it possible in the current study to predict the stability of all 209 PBDE congeners using the GAM and develop a photodegradation model to predict the relative abundances of their photodegradation products.

Although studies on the photodegradation of PBDEs have been conducted, identification of reaction products has been limited and reaction pathways have not been explained in detail [9,10,12–14]. In one of the studies, BDE-209 and 14 other PBDE congeners were shown to undergo first-order photo-

degradation reactions and stepwise loss of bromine [9]. Bezares-Cruz, Jafvert, and Hua proposed a limited reaction pathway for BDE-209 photodegradation to BDE-47 [10].

To better understand PBDE photodegradation and validate the photodegradation model, experiments were conducted on the photodegradation of BDE-209, BDE-184, BDE-100, and BDE-99 under UV light. The congener BDE-209 is the major ingredient of deca-BDE technical mixture, which is still being used in large quantity; BDE-184 is one of the previously unreported products of BDE-209 photodegradation; and BDE-100 and BDE-99 are the major penta-BDEs detected in the environment [3–5]. The stepwise debromination to form lower BDE congeners was monitored and products were identified using gas chromatography–mass spectrometry (GC-MS), a new PBDE GC retention time model, and PBDE standards [15,16]. In the present study, the relative abundances of PBDE photodegradation products from experiments were compared to those predicted by the photodegradation model. Specifically, these calculations and the model indicate that bromine dissociation energy is correlated with the relative photodegradation rate, a relationship that can be used to predict the photodegradation products and their relative abundances.

MATERIALS AND METHODS

Chemicals

A standard mixture of 39 PBDEs was obtained from Cambridge Isotope (Andover, MA, USA) [15]. Individual standards of BDE-99, BDE-100, BDE-121, BDE-140, BDE-146, BDE-148, BDE-168, BDE-184, BDE-196, BDE-197, BDE-203, BDE-206, BDE-207, and BDE-208 were purchased from AccuStandard (New Haven, CT, USA). Standard of BDE-209 was purchased from Aldrich (St. Louis, MO, USA). Some of

* To whom correspondence may be addressed
(staci.simonich@orst.edu).

Published on the Web 7/9/2008.

the PBDE photodegradation products, which were not identified using the preceding standards, were confirmed with an additional 126 individual PBDE congeners [16].

Methods

Ultraviolet photodegradation studies were conducted using a Rayonet RPR-100 photochemical reactor with RMR-2537A (254 nm, 2.7×10^{-8} mol/s/cm³) UV lamps purchased from Southern New England Ultra Violet Company (Branford, CT, USA). The outside of the photoreactor measured 40.6 cm high and 30.5 cm square, the reactor barrel was 25.4 cm in diameter by 38.1 cm deep, and the temperature was approximately 35°C inside the reactor with the fan in operation. Congeners of PBDE were dissolved in 10 ml of isooctane, and these solutions were irradiated in sealed cylindrical quartz vials. Isooctane was chosen as the solvent because the PBDE standards were purchased in isooctane and previous studies in hexane [10] and toluene [12] have shown that organic solvent type does not affect the PBDE debromination pattern [12]. Isooctane has been previously used to study the photodegradation of chlorinated dioxins [17]. Starting concentrations of BDE-99, BDE-100, and BDE-184 were 1 to 10 μmol/L, and the BDE-209 solution was saturated at 196 μmol/L. The irradiated samples were analyzed using a JEOL GC mate II GC high-resolution mass spectrometer in electron capture negative ionization mode (JEOL, Peabody, MA, USA). The GC column was a 30-m J&W DB-5 column (0.25-mm inner diameter and 0.25-μm film thickness, J&W, Folsom, CA, USA), and the GC temperature program was 100°C (hold for 1 min) and then 10°C/min to 320°C (hold for 27 min). The temperatures of the splitless injector, GC interface, and ion source were 280, 250, and 250°C, respectively. The PBDE congeners were quantified using external calibration. These PBDE congeners without available standards were quantified using the average electron capture negative ionization response of the homologous PBDE group.

Multiple linear regression analysis was used to predict the GC retention time of the photodegradation products. The enthalpy of formation (ΔH_f), the number of ortho-, meta-, and para-bromines, polarizability, highest occupied molecular orbital (HOMO) energy, lowest unoccupied molecular orbital (LUMO) energy, dipole moment, and natural logarithm of molecular weight, or $\ln(\text{MW})$, were included in the GC retention time model as molecular descriptors. All molecular descriptors, except for $\ln(\text{MW})$, were obtained using Gaussian 03 [18] on the B3LYP/6-31G(d)//B3LYP/6-31G(d) level, which is more precise than the results obtained by semi-empirical methods [19–21]. Molecular descriptors, such as ΔH_f , polarizability, HOMO, LUMO, and especially dipole moments, are different for different conformational isomers of a given PBDE congener. These molecular descriptors were averaged for PBDE congeners that had more than one stable conformation.

Photodegradation model

The enthalpies of formation of all 209 PBDE congeners were obtained using a previously developed GAM [11]. Briefly, for a specific PBDE congener,

$$\Delta H_f \text{ (kJ/mol)} = 21.979 \cdot \text{BrNumber} + 56.569 + \Delta H_1 + \Delta H_2 + \Delta H_3 \quad (1)$$

where ΔH_1 is the difference in enthalpy between the specific Br position in question and the most stable position on the phenyl ring and ΔH_2 and ΔH_3 are the energies due to repulsion,

respectively, between two bromines on one phenyl ring and between two bromines on opposite phenyl rings [11].

The photodegradation reactions of PBDEs have been reported to be first order [9,13]. In the model developed in the present study, the photodegradation of a PBDE congener is presumed to proceed by detachment of a bromine followed by addition of H from an H-donor. The loss of bromine is the rate-determining step. In the photodegradation of PBDEs, the reaction rate of a specific PBDE congener i is

$$-\frac{d[i]}{dt} = \sum k_i [i] - \alpha_{hi} k_h^i [h] \quad (2)$$

$$\sum k_i = \sum \alpha_{ij} k_j^i \quad (3)$$

In Equation 2, $[i]$ is the concentration of the PBDE congener i , and $\sum k_i$ is the total degradation rate constant for PBDE congener i . Since i can also be a product of higher PBDE congener (h) degradation, the reaction rate of i also included $-\alpha_{hi} k_h^i [h]$ in Equation 2, in which $[h]$ is the concentration of the parent PBDE congener, k_h^i is the rate constant for h degradation to i , and α_{hi} is the number of potential pathways for the degradation of h to i . The $\sum k_i$ is calculated in Equation 3, where k_j^i is the reaction rate constants for i degradation to the lower PBDE j and α_{ij} is the number of potential pathways for the degradation of i to j . For example, in the photodegradation of BDE-209, the reaction rate of BDE-209 is expressed

$$-\frac{d[209]}{dt} = \sum k_{209} \cdot [209] \quad (4)$$

$$\sum k_{209} = 2 \cdot k_{209}^{208} + 4 \cdot k_{209}^{207} + 4 \cdot k_{209}^{206} \quad (5)$$

Similarly, BDE-208, which is one of the products of BDE-209 photodegradation, photodegrades to produce BDE-198, BDE-199, BDE-200, BDE-201, and BDE-202 at the rate

$$-\frac{d[208]}{dt} = \sum k_{208} \cdot [208] - 2 \cdot k_{209}^{208} \cdot [209] \quad (6)$$

where

$$\sum k_{208} = 2 \cdot k_{208}^{198} + 2 \cdot k_{208}^{199} + 2 \cdot k_{208}^{200} + 2 \cdot k_{208}^{201} + k_{208}^{202} \quad (7)$$

The photodegradation rate constant can be calculated from the following expression:

$$k = A \times \exp\left(\frac{-Ea}{RT}\right) \quad (8)$$

where A is a pre-exponential factor, R is the gas constant, T is temperature, and Ea is the bromine dissociation energy. To simplify the model, we assume the A and T are the same for all 209 PBDE congeners; therefore, the rate constant is only correlated to Ea . Also, the positional isomerization that is possible during debromination is not likely to occur because of the excessive energy required. For example, for the two photodegradation pathways BDE-209 to BDE-207 and BDE-209 to BDE-208, the ratio of reaction rates would be

$$\frac{k_{209}^{207}}{k_{209}^{208}} = \exp\left[\frac{-D(\text{C}-\text{Br})_{\text{meta}} + D(\text{C}-\text{Br})_{\text{para}}}{RT}\right] \quad (9)$$

in which $D(\text{C}-\text{Br})_{\text{para}}$ and $D(\text{C}-\text{Br})_{\text{meta}}$ are the bond dissociation energies of para and meta C-Br bonds in BDE-209. The difference in ΔH_f , as given by Equation 1, between BDE-208 and BDE-207 is equivalent to the difference in bond dissociation energies between the para and the meta C-Br bonds of BDE-209:

$$-D(C - \text{Br})_{\text{meta}} + D(C - \text{Br})_{\text{para}} = -\Delta H_{f207} + \Delta H_{f208} \quad (10)$$

in which ΔH_{f207} and ΔH_{f208} stand for the enthalpies of formations of BDE-207 and BDE-208, respectively.

Equation 9 and 10 together give the following:

$$\frac{k_{209}^{207}}{k_{209}^{208}} = \exp\left(\frac{\Delta H_{f207} - \Delta H_{f208}}{-RT}\right) \quad (11)$$

For all PBDEs, a general expression of Equation 11 is

$$\frac{k_h^i}{k_h^j} = \exp\left(\frac{\Delta H_{f_i} - \Delta H_{f_j}}{-RT}\right) \quad (12)$$

Because the model in the present study provides the ratio of the rate constants between different reaction pathways, the photodegradation rate constants are all relative rate constants. To predict the photodegradation of PBDEs in experiments, at least one experimental value of the rate constant must be known. In all cases of the present study, that is the degradation rate constant of the reactant PBDE.

A Visual BASIC program was developed to calculate the relative abundances of reactant and photodegradation products by calculating the change in the concentration over a small time interval:

$$-d[i] = \left(\sum k_i \cdot [i] - \alpha_{hi} k_h [h]\right) dt \quad (13)$$

Using the initial concentration and experimental rate constant of the reactant PBDE, this model estimates the final concentration at a specific reaction time.

RESULTS AND DISCUSSION

Calculated enthalpy of formation of PBDE congeners

We have previously shown that the GAM yields values for ΔH_f that are consistent with those calculated using a density functional theory method in Gaussian 03 at the B3LYP/6-31G(d)//B3LYP/6-31G(d) level for 39 PBDEs [11]. Therefore, ΔH_f for each of the 209 PBDE congeners was calculated using the GAM [11] and are shown in Figure S1 (*Supporting Information*, <http://dx.doi.org/10.1897/07-570.S1>). Among homolog groups, the higher-energy PBDE congeners tend to have more adjacent bromines and more ortho-bromines than other PBDE congeners, for example, BDE-1 (2-monoBDE), BDE-5 (2,3-diBDE), BDE-21 (2,3,4-triBDE), BDE-24 (2,3,6-triBDE), BDE-61 (2,3,4,5-tetraBDE), BDE-62 (2,3,4,6-tetraBDE), BDE-116 (2,3,4,5,6-pentaBDE), BDE-142 (2,2',3,4,5,6-hexaBDE), BDE-173 (2,2',3,3',4,5,6-heptaBDE), and BDE-195 (2,2',3,3',4,4',5,6-octaBDE). However, some PBDE congeners with the highest number of ortho-bromines, for example, BDE-54 (2,2',6,6'-tetraBDE), BDE-96 (2,2',3,6,6'-pentaBDE), and BDE-155 (2,2',4,4',6,6'-hexaBDE), do not have the highest energies. Clearly, repulsion energies, caused by adjacent bromine atoms, make the greatest contribution to ΔH_f within a homologous PBDE group.

In general, the PBDE congeners with the lowest energies among homologs are the congeners with lowest number of adjacent bromines and lowest number of ortho-bromines; examples include BDE-11 (3,3'-diBDE), BDE-13 (3,4'-diBDE), BDE-36 (3,3',5-triBDE), BDE-39 (3,4',5-triBDE), BDE-80 (3,3',5,5'-tetraBDE), BDE-120 (2,3',4,5,5'-pentaBDE), BDE-121 (2,3',4,5,6'-pentaBDE), BDE-155 (2,2',4,4',6,6'-hexaBDE), BDE-184 (2,2',3,4,4',6,6'-heptaBDE), and BDE-197 (2,2',3,3',4,4',6,6'-octaBDE). However, among these examples, BDE-155, BDE-184, and BDE-197 are fully ortho-bro-

minated. Therefore, it appears that ortho-bromine substitution does not contribute to the energy as much as adjacent bromine substitution does.

It should be noted that the most abundant PBDE photodegradation products are not always the most stable congeners. For example, of the penta-BDEs, the ΔH_f for BDE-99 is slightly higher than the ΔH_f for BDE-121 and BDE-120. Nevertheless, experiments show that BDE-99 is the most abundant penta-BDE product resulting from BDE-209 photodegradation [10], which indicates that photodegradation of BDE-209 follows certain reaction pathways and that the stability is not the only factor to decide the relative abundance of the photodegradation products. The possible photodegradation products of PBDE congeners, and their relative abundances, can be predicted from the calculated values of ΔH_f for all 209 PBDEs, assuming that the positional isomerization, which requires substantial energy, does not occur.

GC retention time prediction of photodegradation products

To obtain reliable predictions of GC retention times for photodegradation products, it was necessary to use eight molecular descriptors of physicochemical properties. Specifically, the following linear expression was used to predict GC retention times for PBDE photodegradation products:

$$\begin{aligned} \text{Retention time (min)} &= \beta_0 + \beta_1 \times \Delta H_f + \beta_2 \times \text{polarizability} \\ &+ \beta_3 \times \text{HOMO} + \beta_4 \times \text{LUMO} + \beta_5 \times \ln(\text{MW}) \\ &+ \beta_6 \times \text{ortho bromine} + \beta_7 \times \text{para bromine} \\ &+ \beta_8 \times \text{meta bromine} + \beta_9 \times \text{dipole moment} \quad (14) \end{aligned}$$

where ΔH_f is the enthalpy of formation in kJ/mol; polarizability is the average molecular polarizability in atomic units; HOMO and LUMO are molecular orbital energies in eV; $\ln(\text{MW})$ is the natural logarithm of molecular weight; ortho-bromine, para-bromine, and meta-bromine are the number of bromines at ortho-, para-, and meta-bromines, respectively; dipole moment is the average dipole moment in Debye; and β_0 to β_9 are empirically determined by multiple linear regression, and are, therefore, specific for the DB-5 column and GC temperature program used in the present study. Previous GC retention time models have been used to identify the number of bromines on an unknown PBDE congener [19–21]. However, these models are not precise enough to identify PBDEs within a homologous group. In contrast, values computed from Equation 14 for 47 of the PBDEs (Table S1; <http://dx.doi.org/10.1897/07-570.S1>) show good linearity, between and, in particular, within homologous groups ($R^2 = 0.9939$, $p < 0.0001$; Fig. S2A). The values of β_0 to β_9 in Fig. S2A are -27.3227 , 0.0586 , 0.0027 , -15.6492 , 19.6598 , 5.5465 , -1.1053 , -0.4677 , 0.0141 , and 0.2243 , respectively. A residual plot (Fig. S2B) shows that, with only two exceptions, the predicted GC retention times are within 0.6 min of their corresponding measured retention times and there is no systematic trend. The outliers, BDE-168 (2,3',4,4',5',6-hexaBDE) and BDE-196 (2,2',3,3',4,4',5,6'-octaBDE), have one of the greatest dipole moments (2.33 Debye and 1.74 Debye, respectively) within their homolog groups.

PBDE photodegradation model validation

In a recent study [22], quantitative structure–property relationship models were used to predict the photodegradation

rates of 15 PBDEs based on experimental reaction rate [9]; however, the photodegradation rates for the remaining 194 PBDEs were not predicted. In the present study, the photodegradation rate constants of the 208 PBDE congeners that are potential photodegradation products of BDE-209 were calculated using Equations 3 and 12 relative to an arbitrarily assigned rate constant of 1/min for BDE-209 (Table S2). From among these values, 15 congeners were plotted (Fig. S3) against the corresponding photodegradation rate constants measured in methanol:water (80:20) under UV light [9]. The linear correlation between the experimental rate constants [9] and those predicted from Equations 2 and 13 is good ($R^2 = 0.8958$, $p < 0.0001$; Fig. S3; <http://dx.doi.org/10.1897/07-570.S1>).

Using Equation 13, the abundances of hepta-BDEs relative to total PBDE concentration were computed at different reaction times (Fig. S4; <http://dx.doi.org/10.1897/07-570.S1>). The predicted relative abundance of PBDE congeners was inversely correlated with their ΔH_f at a short reaction time (Fig. S4A compared to the hepta-BDE in Fig. S1). However, at longer reaction times, the congeners with the slowest total degradation rates (Table S2; <http://dx.doi.org/10.1897/07-570.S1>) had the highest relative abundance (BDE-187 and BDE-188; Fig. S4B).

A recent study [13] reported the time profile for the photodegradation products of several PBDE congeners, namely, BDE-47, BDE-100, BDE-99, BDE-154, and BDE-153, coated on a solid-phase microextraction fiber and irradiated with simulated sunlight. Using the rate constants from their study ($\Sigma k_{100} = 0.096/\text{min}$ and $\Sigma k_{153} = 0.401/\text{min}$) [13], we calculated the photodegradation time profile of BDE-100 and BDE-153 (Fig. S5A and B). Using our photodegradation model, we also predicted the photodegradation of BDE-209 from previous studies [10,12]. Using the reported rate constants, the prediction of the solar photodegradation of BDE-209 in hexane [10] is shown in Figure S5C and the prediction of the photodegradation of BDE-209 on silica gel under UV light [12] is shown in Figure S5D. When compared to the corresponding literature results [10,12,13], our photodegradation model predicted PBDE photodegradation time profiles under different conditions (solvent and light conditions) very well.

Photodegradation experiments and model predictions

Using our theoretical model of PBDE photodegradation and GC retention time prediction, we conducted laboratory photodegradation experiments on BDE-209, BDE-184, BDE-100, and BDE-99 to better understand PBDE photodegradation time profiles. The congener BDE-184 has not been previously reported to be a photodegradation product of BDE-209. However, BDE-184 is one of the predicted important BDE-209 photodegradation products (Fig. S4), and the prediction was confirmed experimentally (data not shown). In addition, it was both predicted by the model and experimentally observed that the major products of BDE-184 photodegradation are BDE-154, BDE-155, and BDE-100 (Fig. 1). With only three exceptions, the predicted photodegradation products of BDE-184 after 120 min (Fig. 1C) correlate with the corresponding product peaks in the GC-MS chromatogram from the BDE-184 photodegradation experiment after 120 min of UV irradiation ($R^2 = 0.4882$, $p = 0.0168$ overall and $R^2 = 0.9786$, $p < 0.0001$ without the three exceptions; Figs. S6 and 1D). Two of the exceptions, BDE-139 and BDE-140, were predicted at concentrations much lower than observed, whereas the other ex-

ception, BDE-155, was predicted at a much higher concentration than observed experimentally. The congener BDE-155 (2,2',4,4',6,6'-hexaBDE) is fully brominated in the ortho positions. The stability of the ortho-bromine may be overpredicted by the model, which results in higher predicted concentrations relative to the experiment. All of the major chromatographic peaks in Figure 1D were identified using PBDE standards except for the two peaks at 19.95 and 23.05 min. The chromatographic peak at 19.95 min was predicted to be BDE-103 based on the GC retention time model (Table S1) and photodegradation model (Fig. 1C); the peak at 23.05 min was assigned as BDE-139, which has a predicted retention time of 22.88 min. The identities of BDE-103 and BDE-139 were confirmed using the 126 PBDE standards [16].

The photodegradation of BDE-100 and BDE-99, which are the most abundant penta-BDEs detected in the environment [3–5], has been previously studied [9,13]. However, not all of the products were identified and the reaction mechanism was not explained in detail. Therefore, we also studied the photodegradation of these important penta-BDEs. The experimentally determined time profile for the photodegradation of BDE-100 (Fig. S7A) was predicted from the photodegradation model in all but one case (BDE-28; Fig. S7B). Compared to all other BDE-100 photodegradation products with two or more ortho-bromines, BDE-28 (2,4,4'-triBDE) only has one bromine in the ortho position. The stability of the ortho-bromine may be overpredicted by the model, which results in higher predicted concentrations relative to the experiment, except for BDE-28. As was observed in the photodegradation of BDE-184, the total concentration of PBDEs decreased with time.

The most abundant photodegradation products of BDE-100 at 10 min were predicted from the photodegradation model to be BDE-75, BDE-47, and BDE-28 (Fig. S7C); these predictions corresponded to the most abundant photodegradation products observed in the GC-MS chromatogram of a BDE-100 sample after 10 min of irradiation (Fig. S7D). All major chromatographic peaks were identified using PBDE standards except for the peaks at 18.16 and 18.55 min (which co-elute with BDE-75). A recent study [16] showed that BDE-75 and BDE-51 co-elute and, further, that BDE-50 has a shorter retention time than BDE-51 on a DB-5 column under a GC temperature program similar to the one used in the present study. Based on this information and photodegradation model, the peaks at 18.16 and 18.55 min are most likely BDE-50 and BDE-51, respectively. The identities of BDE-50 and BDE-51 were confirmed using the 126 PBDE standards [16]. Linear correlation between the experimental concentrations and those concentrations predicted by the model for the photodegradation of BDE-100 after 5 min of irradiation is good ($R^2 = 0.7892$, $p = 0.0180$; Fig. S8).

For BDE-99, the photodegradation model predicted that the four primary products, BDE-66, BDE-74, BDE-47, and BDE-49, reached their maximum concentrations after approximately 2 min of irradiation (Fig. S9); this result closely matched the experiment (Fig. S9A). Again, the total concentration of PBDEs in the BDE-99 photodegradation experiment decreased significantly with time after 5 min of irradiation.

As was true for BDE-100 photodegradation, all predicted major photodegradation products of BDE-99 at 5 min (Fig. S9C) appeared in the GC-MS chromatogram of a BDE-99 sample irradiated for 5 min (Fig. S9D). The chromatographic peaks at 16.21, 16.67, and 19.20 min were predicted to be

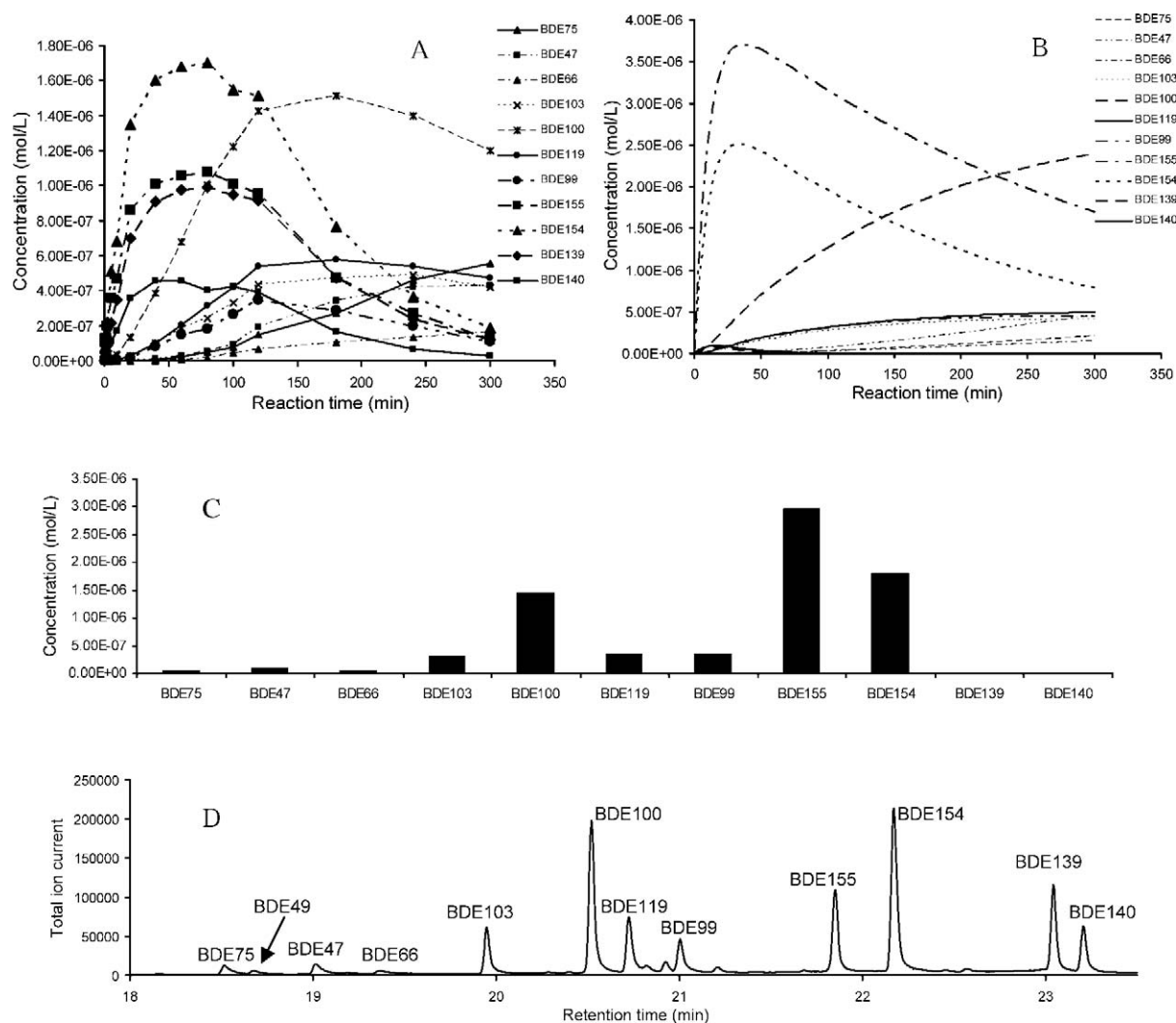


Fig. 1. Photodegradation of BDE-184 in isooctane under ultraviolet light: Experimental results (A), model prediction (B). Model prediction (C) and experimental results (D) of BDE-184 photodegradation at 120 min. BDE = brominated diphenyl ether.

BDE-18, BDE-31, and BDE-74, respectively, based on the GC retention time model prediction of 15.65, 16.31, and 18.96 min, respectively. The identities of BDE-18, BDE-31, and BDE-74 were confirmed by the 126 PBDE standards [16]. The correlation between the experimental concentrations and the predicted concentrations of BDE-99's photodegradation products after 5 min of irradiation did not have good linearity but was statistically significant ($R^2 = 0.4441$, $p = 0.0133$; Fig. S10).

Figure 2A shows the experimental result of the time profile of BDE-209 photodegradation by homologous group. The predicted time profile of BDE-209 photodegradation was calculated and is shown in Figure 2B. After 8 d of irradiation, only 0.16% of mono-BDEs and 0.02% of di-BDEs were detected in the solution. At the level of homologous group, the theoretical model reproduced the results of the experiment well and both show stepwise debromination of PBDEs over time. The experimental results (Fig. 2C) and model prediction (Fig. 2D) at congener level for penta-BDE and tetra-BDE products indicate that, at the congener level, the model did not predict as well as it did for BDE-184, BDE-100, and BDE-99. Furthermore, the concentrations of the tetra-BDEs were underestimated by the model (Fig. 2E and F), and the correlation between model and experiment also confirmed this (Fig. S11).

Because the photodegradation of BDE-209 has up to ten steps of debromination and could result in 208 possible products, the estimation error may accumulate for each step of debromination and lead to relatively large error.

Photodegradation pathways

The major photodegradation pathways mapped out in the present study for BDE-209, BDE-184, BDE-100, and BDE-99 are summarized in Figure 3. The thicker lines pass through those photodegradation products with higher concentrations; these pathways are more probable than the rest. The relative abundances of photodegradation products were concluded from the experimental results when the model prediction did not agree well with the experimental results. For the photodegradation of BDE-209, BDE-99 is the most abundant penta-BDE product even though it is not the most stable penta-BDE, because it is on the pathway of the highest probability for each step. Similarly, BDE-28 is on the pathway of the highest probability in the photodegradation of BDE-100; therefore, it is the most abundant tri-BDE product.

In all photodegradation experiments conducted, the total amount of PBDEs was observed to decrease with time. This is contradictory to the photodegradation model that assumes constant mass balance. It is possible that the ether bond breaks

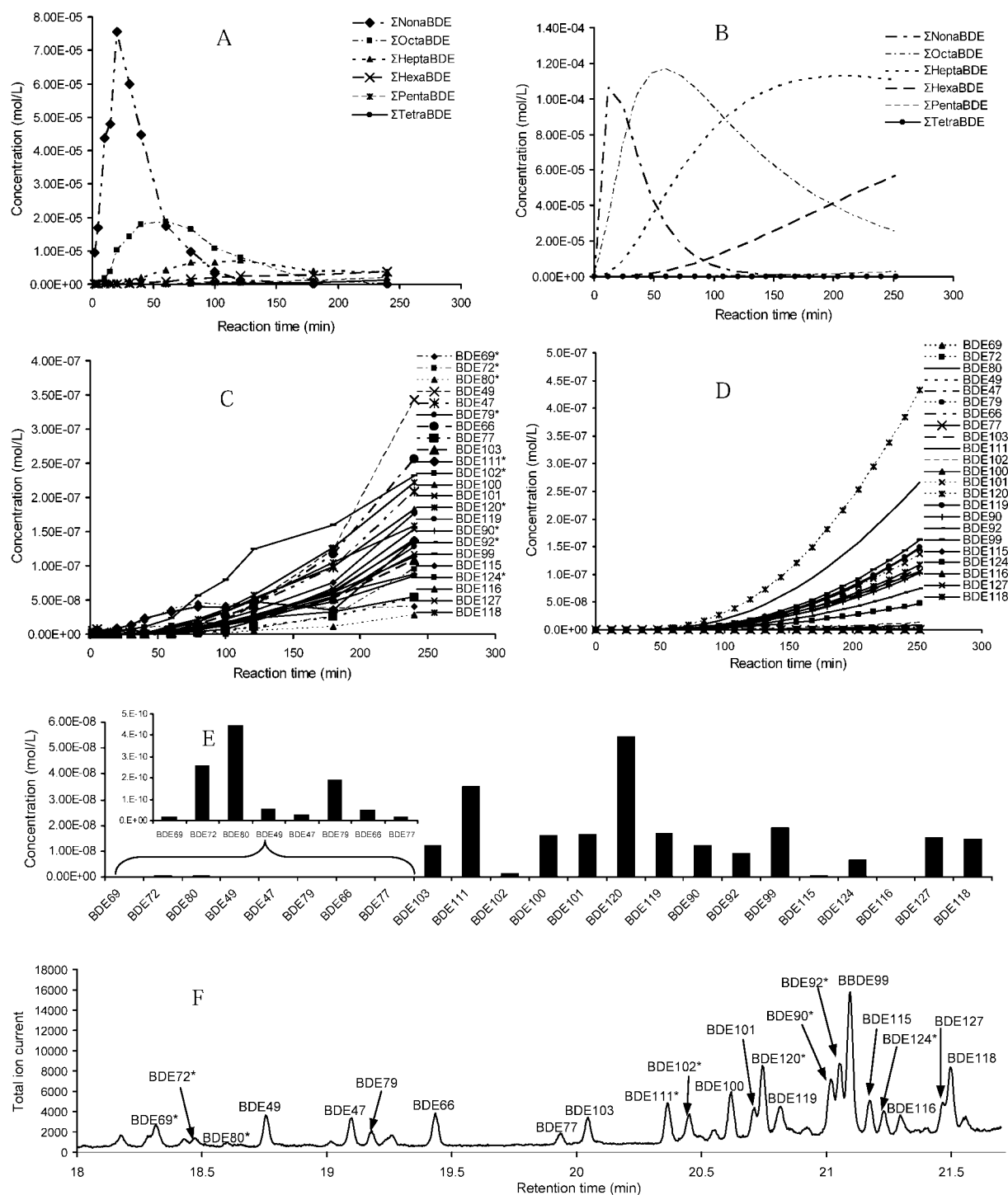


Fig. 2. Photodegradation of BDE-209 in isoctane under ultraviolet light: Experimental results (A) and model prediction (B) by homologous groups. Experimental results (C) and model prediction (D) by congener for penta-BDE and tetra-BDE products. Model prediction (E) and experimental results (F) of BDE-209 photodegradation at 120 min. Asterisk (*) represents polybrominated diphenyl ether congeners not identified by standards. BDE = brominated diphenyl ether.

under UV light, resulting in an apparent loss of PBDE mass [23]. Also, PBDEs may have accumulated on the walls of the reaction tubes and/or polybrominated dibenzo-*p*-furans may have been formed, but were not detected, during the photo reaction. In addition, electron capture negative ionization is not as sensitive for mono- and di-BDEs as other higher-brominated PBDEs [15] and mono- and di-BDEs were rarely detected among the photodegradation products. As a result,

mono- and di-BDEs may not be fully accounted for in the mass balance of the experiments.

The PBDE photodegradation model is a simple model based on the GAM, an approximation to calculate the ΔH_f of PBDEs. Enthalpy of formation may not be the only factor determining the PBDE photodegradation rate constant. Other factors may include quantum yield, molecular orbital energy, and charge distribution [22]. The quantum yield for PBDE photodegra-

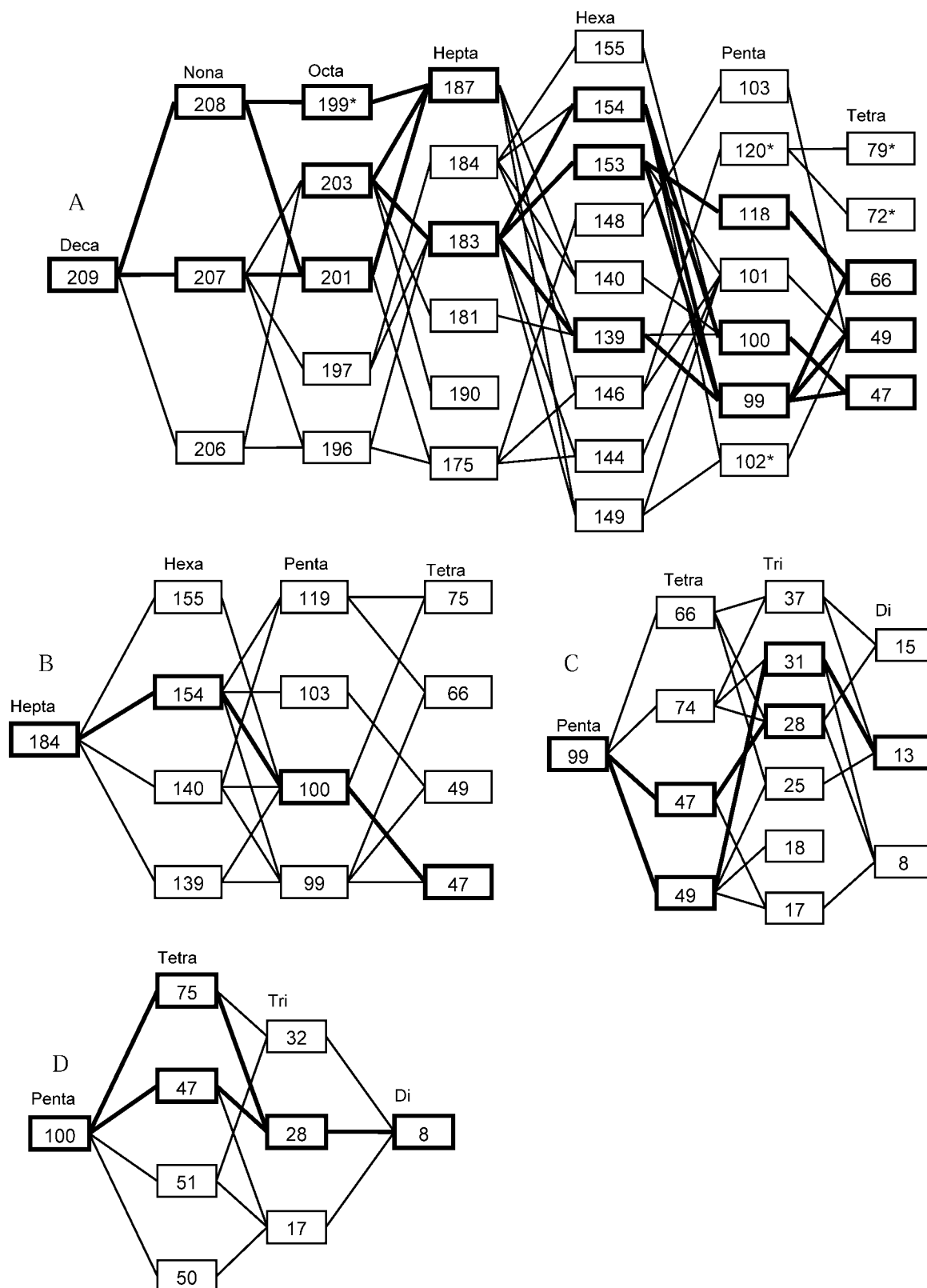


Fig. 3. Reaction pathways of brominated diphenyl ether (BDE)-209 (A), BDE-184 (B), BDE-99 (C), and BDE-100 (D) photodegradation. The thicker lines pass through those photodegradation products with higher concentrations. Only major BDE-209 pathways are shown. Asterisk (*) represents polybrominated diphenyl ether congeners not confirmed by standards.

dition was assumed to be constant. Furthermore, the model assumes that the solvent effect and light conditions have the same effect on all PBDE congeners. These limitations may cause the observed deviations from the experimental results.

However, good linear correlation was observed between our predicted photodegradation rates (relative to BDE-209) and experimental photodegradation rates in methanol:water under 365 nm of UV light. Our photodegradation model predicted

PBDE photodegradation time profiles under different solvent and light conditions very well when compared to the experimental results [10,12,13]. This photodegradation model is not wavelength or solvent specific. Therefore, our model can be used to predict PBDE photodegradation under environmentally relevant conditions.

Previous studies have shown that the current PBDE congeners in the environment are similar to the congener composition of the technical mixtures used [3,4]. Assuming that most of the BDE-209 in the environment is eventually photodegraded by natural sunlight, the future pattern of the PBDE congeners caused by BDE-209 degradation in the environment may be comparable to our results. For example, BDE-99 will remain the most abundant penta-BDE, while BDE-49 and BDE-66 will increase greatly and will be comparable in abundance to BDE-47. It is also possible that PBDE congeners that have not been used commercially, such as octa-BDE-201 and hepta-BDE-187, will be present in the environment at significant concentrations among their congener group.

SUPPORTING INFORMATION

Table S1. Experimental and multiple linear fit GC retention times for PBDE congeners.

Table S2. Calculated reaction rate constants relative to BDE-209 for all 209 PBDEs.

Fig. S1. Enthalpy of formation of 209 PBDEs calculated using the GAM [1].

Fig. S2. Correlation between measured and predicted GC retention time (A) and plot of residuals (B).

Fig. S3. Correlation between predicted photodegradation rates (relative to BDE-209) and experimental rates [2].

Fig. S4. Predicted hepta-BDE products from BDE-209 photodegradation in methanol:water (80:20) and UV light: the product profile at $1 \times 10_5$ sec reaction time (A), and the product profile at $1.4 \times 10_6$ sec (B). The concentrations are relative to the total BDE concentration.

Fig. S5. Predicted PBDE photodegradation time profiles. Predicted photodegradation of BDE-100 (A) and BDE-153 (B), respectively, after solid-phase microextraction fiber exposure to sunlight simulated irradiation normalized to the maximum concentration of each homologous group [3]. Predicted solar photodecomposition of BDE-209 (C) in hexane relative to total PBDE concentration [4]. Predicted photodegradation of BDE-209 (D) on silica gel under UV light relative to total PBDE concentration [5].

Fig. S6. Correlation between experimental concentration and model predicted concentration for BDE-184 photodegradation products at 120 min.

Fig. S7. Photodegradation of BDE-100 in isoctane under UV: experimental results (A) and model prediction (B) for BDE-100. Model prediction (C) and experimental results (D) of BDE-100 photodegradation at 5 min.

Fig. S8. Correlation between experimental result and model simulation for BDE-100 photodegradation products at 5 min.

Fig. S9. Photodegradation of BDE-99 in isoctane under UV: experimental results (A) and model prediction (B) for BDE-99. Model prediction (C) and experimental results (D) of BDE-99 photodegradation at 5 min.

Fig. S10. Correlation between experimental result and model simulation for BDE-99 photodegradation products at 5 min.

Fig. S11. Correlation between experimental result and model simulation for tetra-BDEs and penta-BDEs in BDE-209 photodegradation products at 120 min.

All found at DOI: 10.1897/07-570.S1 (173 KB PDF).

Acknowledgement—This publication was made possible in part by grant P30ES00210 from the National Institute of Environmental Health Sciences, National Institutes of Health, through a pilot project awarded by Oregon State University's Environmental Health Sciences Center. Its contents are solely the responsibility of the authors and do not necessarily represent the official view of the National Institute of Environmental Health Sciences or the National Institutes of Health. The authors would like to acknowledge Oregon State University's Environmental Health Sciences Center's mass spectrometry core facility for assistance, as well as Max Deinzer, Luke Ackerman, and the Oregon State University Department of Chemistry Harris Fellowship.

REFERENCES

- Hale RC, La Guardia MJ, Harvey E, Mainor TM. 2002. Potential role of fire retardant-treated polyurethane foam as a source of brominated diphenyl ethers to the US environment. *Chemosphere* 46:729–735.
- de Wit CA. 2002. An overview of brominated flame retardants in the environment. *Chemosphere* 46:583–624.
- Hites RA. 2004. Polybrominated diphenyl ethers in the environment and in people: A meta-analysis of concentrations. *Environ Sci Technol* 38:945–956.
- Elliott JE, Wilson LK, Wakeford B. 2005. Polybrominated diphenyl ether trends in eggs of marine and freshwater birds from British Columbia, Canada, 1979–2002. *Environ Sci Technol* 39:5584–5591.
- Dodder NG, Strandberg B, Hites RA. 2002. Concentrations and spatial variations of polybrominated diphenyl ethers and several organochlorine compounds in fishes from the northeastern United States. *Environ Sci Technol* 36:146–151.
- Madia F, Giordano G, Fattori V, Vitalone A, Branchi I, Capone F, Costa LG. 2004. Differential in vitro neurotoxicity of the flame retardant PBDE-99 and of the PCB Aroclor 1254 in human astrocytoma cells. *Toxicol Lett* 154:11–21.
- Muirhead EK, Skillman AD, Hook SE, Schultz IR. 2006. Oral exposure of PBDE-47 in fish: Toxicokinetics and reproductive effects in Japanese Medaka (*Oryzias latipes*) and fathead minnows (*Pimephales promelas*). *Environ Sci Technol* 40:523–528.
- Hale RC, Alaae M, Manchester-Neesvig JB, Stapleton HM, Ikononou MG. 2003. Polybrominated diphenyl ether flame retardants in the North American environment. *Environ Int* 29:771–779.
- Eriksson J, Green N, Marsh G, Bergman A. 2004. Photochemical decomposition of 15 polybrominated diphenyl ether congeners in methanol/water. *Environ Sci Technol* 38:3119–3125.
- Bezales-Cruz J, Jafvert CT, Hua I. 2004. Solar photodecomposition of decabromodiphenyl ether: Products and quantum yield. *Environ Sci Technol* 38:4149–4156.
- Zeng X, Freeman PK, Vasil'ev YV, Voinov VG, Simonich SL, Barofsky DF. 2005. Theoretical calculation of thermodynamic properties of polybrominated diphenyl ethers. *J Chem Eng Data* 50:1548–1556.
- Soderstrom G, Sellstrom U, de Wit CA, Tysklind M. 2004. Photolytic debromination of decabromodiphenyl ether (BDE 209). *Environ Sci Technol* 38:127–132.
- Sanchez-Prado L, Lores M, Llompart M, Garcia-Jares C, Bayona JM, Cela R. 2006. Natural sunlight and sun simulator photolysis studies of tetra- to hexa-brominated diphenyl ethers in water using solid-phase microextraction. *J Chromatogr A* 1124:157–166.
- Barcellos da Rosa M, Krüger H-U, Thomas S, Zetzsch C. 2003. Photolytic debromination and degradation of decabromodiphenyl ether, an exploratory kinetic study in toluene. *Fresenius Environ Bull* 12:940–945.
- Ackerman LK, Wilson GR, Simonich SL. 2005. Quantitative analysis of 39 polybrominated diphenyl ethers by isotope dilution GC/low-resolution MS. *Anal Chem* 77:1979–1987.
- Korytar P, Covaci A, de Boer J, Gelbin A, Brinkman UA. 2005. Retention-time database of 126 polybrominated diphenyl ether congeners and two bromkal technical mixtures on seven capillary gas chromatographic columns. *J Chromatogr A* 1065:239–249.
- Kieatwong S, Nguyen LV, Hebert VR, Hackett M, Miller GC, Mielle MJ, Mitzel R. 1990. Photolysis of chlorinated dioxins in organic solvents and on soils. *Environ Sci Technol* 24:1575–1580.
- Gaussian. 2003. *Gaussian 03, Rev B.05*. Pittsburg, PA, USA.
- Rayne S, Ikononou MG. 2003. Predicting gas chromatographic

- retention times for the 209 polybrominated diphenyl ether congeners. *J Chromatogr A* 1016:235–248.
20. Harju M, Andersson PL, Haglund P, Tysklind M. 2002. Multivariate physicochemical characterisation and quantitative structure–property relationship modelling of polybrominated diphenyl ethers. *Chemosphere* 47:375–384.
 21. Wang Y, Li A, Liu H, Zhang Q, Ma W, Song W, Jiang G. 2006. Development of quantitative structure gas chromatographic relative retention time models on seven stationary phases for 209 polybrominated diphenyl ether congeners. *J Chromatogr A* 1103:314–328.
 22. Niu J, Shen Z, Yang Z, Long X, Yu G. 2006. Quantitative structure–property relationships on photodegradation of polybrominated diphenyl ethers. *Chemosphere* 64:658–665.
 23. Hageman HJ, Louwerse HL, Mijs WJ. 1970. Photoreactions of some diaryl ethers. *Tetrahedron* 26:2045–2052.